Some Parameter Characteristics of Thermally Treated Viscose Fibers

I. M. Fouda, A. H. Oraby, E. A. Seisa

Physics Department, Faculty of Science, Mansoura University, Mansoura, Egypt

ABSTRACT: This article sheds light on some structural changes in thermally treated viscose fibers at a constant temperature of $100 \pm 1°C$ at different time periods. The obtained optical parameters were used to calculate the crystallinity, density, Herman's orientation function, average orientation, and form birefringence. In addition, the stress optical coefficients, thermal stress, molar refractivity, specific refractivity, and polarizabilities along and across the axis and segment anisotropy were obtained. Measurements of the refractive indices helped us to calculate the dielectric constant, dielectric susceptibility, surface reflectivity, and transparency transmittances. The mechanisms of structural variation for the viscose fibers due to the annealing process were examined with the structural details for optothermal parameters. The relationships between the measured and calculated parameters are given in illustrations and curves. © 2010 Wiley Periodicals, Inc. J Appl Polym Sci 118: 1306–1312, 2010

Key words: annealing; density; fibers; optics; thermal properties

INTRODUCTION

Optical parameters, such as the refractive indices and birefringence (Δn), have recently been accepted in general as good indicator parameters of molecular orientation. The crystallinity (χ_c), density (ρ), dielectric constant (d), and other structural parameters all describe the functional behavior of the manufactured fiber properties. Viscose fibers have been recognized as one of the important man-made commercial fibers. Rayon is a general term for man-made filaments prepared from various solutions of modified cellulose. In the case of viscose rayon, the cellulose is brought into solution as cellulose xanthate and is dissolved in an alkaline solution. Viscose is prepared by a wet-spinning process, in which the solidification of the filaments takes place in a fluid acid bath. In this process, a solid skin is first formed, followed by the solidification of the inner portion of the filament. This results in the contraction of the fiber during the spinning process and the formation of folds or lobes on the surface.[1] Its structural and physical properties have been investigated under various conditions. Improvements in the properties of viscose fibers have been due to different thermal and drawing treatments.[2–8]

The process of annealing close to the melting point leads to partial melting and increases chain mobility.[9] Part of the modern trend in fiber research is to alter the fiber properties; one of the methods of property modification involves annealing. Several studies have reported the effect of annealing on the structure of synthetic and natural fibers.[10–17] Annealing may be performed with the ends of the sample free or fixed. In the former case, the sample shrinks, whereas, in the latter case, it retains its length but exerts measurable refractive forces on its fixed ends. Therefore, annealing provides materials with new physical properties to expand their industrial applications.[18]

The principal aim of this study was to examine the changes in the optical results of viscose fiber samples annealed under different conditions with the two-beam interferometry method to calculate the molecular orientation parameters, χ_c, form birefringence (Δn_f), stress optical coefficient (C_s), and other essential parameters.

THEORETICAL CONSIDERATIONS

The two-beam interference technique was used extensively elsewhere[19] to determine optical parameters such as the refractive indices ($n^{\parallel}$ and $n^{\perp}$, where $n^{\parallel}$ and $n^{\perp}$ are the mean refractive indices for the light beam along and across the axis of the fiber, respectively) and Δn for viscose fibers.

Herman's orientation function [$f(\theta)$]

Herman represented $f(\theta)$ by a series of spherical harmonics (Fourier series) as follows:[20]

Correspondence to: E. A. Seisa (seisa@mans.edu.eg).

$$f(\theta) = \sum_{n=0}^{\infty} \left(n + \frac{1}{2}\right) \langle f_n \rangle f_n(\theta) \qquad (1)$$

The odd components were all zero, and the first three even components were given by $f_2(\theta)$, $f_4(\theta)$, and $f_6(\theta)$. The parameter $\langle f_n \rangle$ represents the average amplitude values. A sample of an $f(\theta)$ proportional to Δn is given in the following equation:[21]

$$f_\Delta(\theta) = \Delta n / \Delta n_{\max} \qquad (2)$$

where $f_\Delta(\theta)$, optical orientation function; $\Delta n_{\max}$ is the maximum birefringence of a fully oriented fiber.[22]

Average optical orientation

The overall orientation [average optical orientation function (F_{av})] was calculated with Δn measurements on individual fibers. Optical Δn gives the average of the crystalline and amorphous orientations. The term *orientation* frequently means the orientation of ordered phases. It is strongly emphasized, however, that both crystalline and amorphous materials can exist in both oriented and nonoriented states. F_{av} was calculated according to the following equation:[23]

$$F_{av} = 2\Delta n / \left(\Delta n_c^o + \Delta n_a^o\right) \qquad (3)$$

where Δn is the birefringence for the viscose fibers under experimental investigation, Δn_c^o is the birefringence of the crystalline phase ($\Delta n_c^o = 0.0877$), Δn_a^o is the birefringence of the amorphous phase ($\Delta n_a^o = 0.0347$), and $\Delta n_{\max} = 0.055$.[22]

Determination of Δn_f

The total birefringence (Δn_t) of a fiber is the sum of three terms:

$$\Delta n_t = \chi_c \Delta n_c^o + (1 - \chi_c)\Delta n_a^o + \Delta n_f \qquad (4)$$

where χ_c is the crystallinity.[24] Δn_f is a phenomenon arising from the interfaces between the crystalline and amorphous regions.

C_s

The value of C_s is dependent on the chemical structure of the polymer. Furthermore, the value of this coefficient depends on the mean refractive index ($\overline{n}$) and the optical anisotropy of the random link, as shown in the following equation:[25]

$$C_s = \frac{2\pi}{45KT}\left[\frac{\left(\overline{n^2} + 2\right)^2}{\overline{n}}\right]\left[\alpha^\| - \alpha^\perp\right] \qquad (5)$$

where K is Boltzmann's constant, T is the absolute temperature, and $\alpha^\|$ and $\alpha^\perp$ are the polarizabilities along and across the axis of such units, respectively.

Isotropic refractive index (n_{iso})

Because most macromolecular crystals are birefringent, an appropriate average refractive index must be used, as given in the following equation:[26]

$$n_{iso} = (n^{\perp 2} n^\|)^{1/3} \qquad (6)$$

Segment anisotropy (γ_s)

γ_s is related to C_s, which leads to the following equation:[27]

$$C_s = \frac{\gamma_s}{90\psi KT}\frac{\left(\overline{n^2} + 2\right)^2}{\overline{n}} \qquad (7)$$

where ψ is the permittivity of free space (8.85×10^{-12} F/m).

Determination of the thermal stress (σ)

From the calculated value of C_s and the birefringence (Δn), we can obtain σ deformation from the following equation:

$$C_s = \frac{\Delta n}{\sigma} \qquad (8)$$

Calculation of d and the dielectric susceptibility (η)

d is revealed through the following relation:[28]

$$d_\| = \frac{1 + 2(n_\|^2 - 1)/(n_\|^2 + 2)}{1 - (n_\|^2 - 1)/(n_\|^2 + 2)} \qquad (9)$$

where $d_\|$ is the dielectric constant when using monochromatic light vibrating parallel to the fiber axis.

An analogous equation holds for $d_\perp$, dielectric constant when using monochromatic light vibrating perpendicular to the fiber axis. η is related to d through the following well-known equation:

$$\eta = \frac{d - 1}{4\pi} \qquad (10)$$

Molar refractivity (R)

The polarizability of a molecule is related to its refractive index through the Lorentz–Lorenz relation:[28]

$$\frac{\overline{n^2} - 1}{\overline{n^2} + 2}\left(\frac{M}{\rho}\right) = R \qquad (11)$$

where ρ is the density and M is the monomer molecular unit (molar weight = 162.14) for the viscose fibers.

Specific refractivity

The specific refractivities of the isotropic dielectrics ($\varepsilon^{\parallel}$ and $\varepsilon^{\perp}$ in cm^3/g) are proportional to the ρ (g/cm^3) of the medium as given by the De Vries equations:[29]

$$\varepsilon_{\parallel} = (n_{\parallel}^2 - 1)\rho^{-1}/[n_{\parallel}^2 + 2 + S(n_{\parallel}^2 - 1)] \quad (12a)$$

$$\varepsilon_{\perp} = (n_{\perp}^2 - 1)\rho^{-1}/[n_{\perp}^2 + 2 - 1/2S(n_{\perp}^2 - 1)] \quad (12b)$$

where S is the anisotropy index, which equals 0.07 for viscose fibers.[29]

Calculation of the surface reflectivity ($\overline{R}$)

$\overline{R}$ of a polymer for light at normal incidence can be estimated from Fresnel's equation[28] and $\overline{n}$. Thus, the reflection ($\overline{R}$; in air) is given by

$$\bar{R} = \left(\frac{\overline{n} - 1}{\overline{n} + 1}\right)^2 \times 100 \quad (13a)$$

The transmittance (τ_i) can be given from the following equation (transmittance transparency):

$$\tau_i = 1 - \bar{R} \quad (13b)$$

EXPERIMENTAL

Materials

A viscose fiber solution is a solution of sodium cellulose dithiocarbonate produced from cellulose that has a chemical formula of $(C_6 H_{10} O_5)_n$. Expressed in a structural formula, the viscose solution or cellulose xanthate is as follows:[30]

$$S=C \begin{cases} O\text{-}(C_6 H_9 O_4)_x \\ \\ S\text{-}Na \end{cases}$$
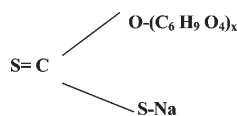
Annealing of the samples

The viscose fibers, manufactured by Misr Rayon (Cairo, Egypt), were distributed in cocoon form on glass rods with free ends, which were then heated in an electric oven at a constant temperature of 100 $\pm$ 1°C at different annealing times, ranging from 15 to 70 min, and then cooled in air. The constant temperature of 100°C was selected because it was above the glass-transition temperature and below the melting temperature. The cross section of viscose fibers was witnessed through an optical microscope and was found to be of irregular shape; the area of one fiber was 1.165×10^{-3} mm^2.

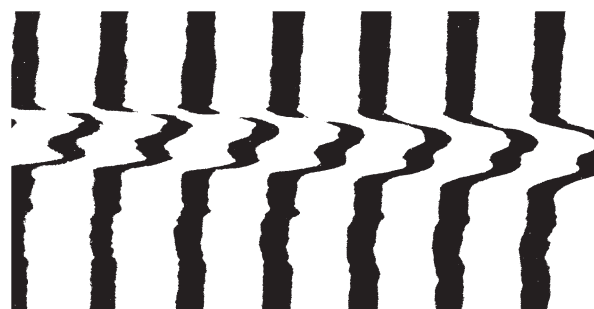**Figure 1** Two-beam interferometery microinterferograms from the totally duplicated image for the viscose fibers at an annealing time of 30 min.

Double-beam interferometry

A viscose fibers Misr Rayon Company (Egypt), was examined by a double-beam Pluta polarizing interference microscope. The microscope was adjusted first to show the total duplicated image of the examined fiber, where the two fringe shifts for light vibrated parallel and perpendicular to the fiber axis. The accuracy of the optical path length difference with a fringe field (Wollaston prism) of the manual standard Pluta polarizing microscope was about $\pm 20 \times 10^{-3}$ λ, wavelength of the monochromatic light used;[19,31] therefore, the error in the determination of the refractive indices was found to be less than $\pm 10^{-3}$, and the accuracy of the fiber thickness was about ± 1 μm.[19,31]

Figure 1 shows an example of the obtained microinterferogram of two-beam interferometry from the total duplicated image of the viscose fibers at an annealing time of 30 min at the constant temperature of 100°C. Both plane polarized light of $\lambda = 546$ nm vibrating along and across the fiber axis and the liquid of refractive index ($n_L = 1.527$) at 21 ± 0.05°C were used.

χ_c

As well-known, n_{iso}[32] is linearly proportional to ρ; this ρ showed a linear dependence on χ_c, as given in the following equation:[6]

$$\chi_c = (n_{iso} - 1.5077)/0.0456 \quad (14)$$

This equation assists researchers in evaluating χ_c from n_{iso}, where the values of $n_{iso} = 1.5077$ ($\chi_c = 0\%$) and $n_{iso} = 1.5533$ ($\chi_c = 100\%$).

ρ equation

ρ was determined through the following equation on the basis of the well-known relation of χ_c:

$$\rho = \chi_c(\rho_c - \rho_a) + \rho_a \quad (15)$$

where ρ_a and ρ_c are the densities of the amorphous and crystalline phase, $\rho_c = 1.625$[26] and $\rho_a = 1.489$ g / cm^3.
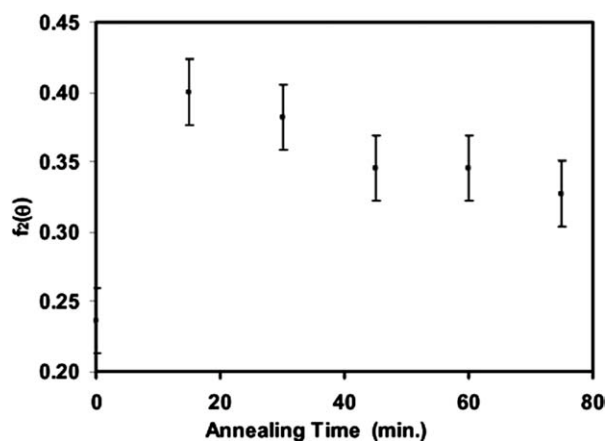
Figure 2 Relationship between $f_2(\theta)$ and the annealing times at a constant annealing temperature for the viscose fibers.
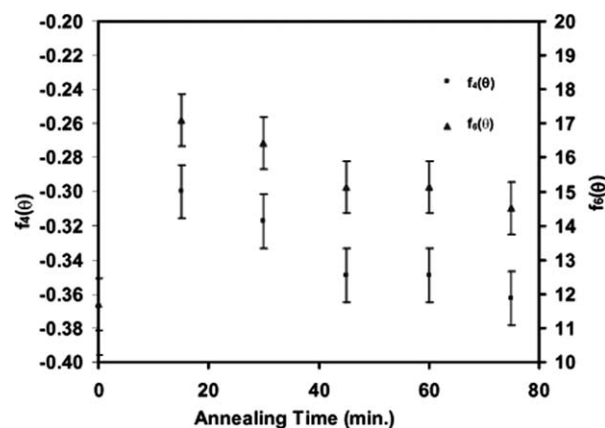

Figure 3 Relationship between $f_4(\theta)$ and $f_6(\theta)$ and the annealing time at a constant annealing temperature for the viscose fibers.

RESULTS

In view of the relevance of the optical $f(\theta)$'s given by Herman's equation with the annealing times, the possibility of explaining the deformation mechanism unfolded. The optical Δn gave a direct measure of these parameters on the basis of the aggregate model, whereas the calculated values for these $[f(\theta)]$'s were useful in predicting the optical parameters of the viscose fibers. Figures 2 and 3 show the relationship between the orientation functions $f_2(\theta)$, $f_4(\theta)$, and $f_6(\theta)$ with different annealing times at the constant temperature for the viscose fibers. The amount of disorientation of a noncrystalline chains depends on the annealing temperature and time. Therefore, it was likely that the disorientation process was a consequence of the thermal energy transferred to the viscose medium. The thermal energy gained because of the temperature and time of heating gave a certain degree of disorientation, as observed at longer times and a constant temperature.

Table I illustrates some experimental results for the apparent volume fraction of crystallinity (χ) and ρ. Also, the calculated values of n_{iso}, $\alpha^{\parallel}$, and $\alpha^{\perp}$ of the monomer unit, and $\overline{R}$ at different annealing times at a constant temperature for the viscose fibers are given. Similarly, in Table II, the calculated values of C_s, σ, $\varepsilon^{\parallel}$, $\varepsilon^{\perp}$, and R at different annealing times

are given for the viscose fibers. Figure 4 shows the relationship between F_{av} and the annealing time at a constant temperature for the viscose fibers. It was clear that the average orientation behavior was similar to $f_2(\theta)$.

Figures 5–8 show the relations among Δn_f, γ_s, average dielectric constant (d_{av}), and average dielectric susceptibility (η_{av}) at different annealing times and a constant temperature. As shown in these figures, Δn_f, γ_s, d, and η all decreased as the annealing time increased.

DISCUSSION

The development of structure reorientation in viscose fiber is a continuing area of technological and scientific study. Heat-treatment operations are important commercial processing steps. These steps produce the structure required for good dying abilities and appearance properties. One of the most available techniques for changing the viscose structure is the heat-treatment process. The effects of the annealing process increase dramatically with time but also depend on the temperature at which the sample is maintained. Like most regenerated cellulose under the influence of heat and light, they show a rapid loss in strength. Short heating at $100 \pm 1°C$ temperatures is less harmful than long heating at the same temperature, as shown in Tables I and II. Δn

TABLE I
Values of χ_c, ρ, n_{iso}, $\alpha^{\parallel}$, $\alpha^{\perp}$, and $\overline{R}$ with Annealing Time for the Viscose Fibers

Annealing time (min)	χ	ρ (g/cm^3)	n_{iso}	$\alpha^{\parallel} \times 10^{-39}$	$\alpha^{\perp} \times 10^{-39}$	$\overline{R}$
Unannealed	0.3206	1.5326	1.5223	1.4434	1.4138	2.2164
15	0.3640	1.5385	1.52433	1.4559	1.4061	2.2398
30	0.3568	1.5375	1.5240	1.4546	1.4070	2.2362
45	0.3642	1.5385	1.5243	1.4514	1.4083	2.2362
60	0.3642	1.5385	1.5243	1.4514	1.4083	2.2362
75	0.3569	1.5375	1.5240	1.4501	1.4092	2.2326

TABLE II
Values of C_s, σ, $\varepsilon^{\parallel}$, $\varepsilon^{\perp}$, and R with Annealing Time for the Viscose Fibers

Annealing time (min)	$C_s \times 10^{-20}$ (Pa^{-1})	$\sigma \times 10^{18}$ (Pa)	$\varepsilon^{\parallel}$	$\varepsilon^{\perp}$	R
Unannealed	1.2492	1.0406	0.1976	0.2020	32.283
15	2.1060	1.0446	0.1992	0.2009	32.261
30	2.0115	1.0440	0.1991	0.2010	32.265
45	1.8188	1.0447	0.1986	0.2012	32.261
60	1.8188	1.0447	0.1986	0.2012	32.261
75	1.7242	1.0440	0.1985	0.2014	32.265

changes in a bulk material of the crystalline, amorphous, form, and thermal energy stress are given as the sum of orientational Δn.

This study revealed the finer details of multiphase systems, such as the fact that semicrystalline viscose fiber should be considered from the contributions of the respective phases. Δn_f is usually neglected, but additional information on Δn_f is required when two-phase systems are involved.[26] If the sign of Δn in the spherulite is positive, this means that the refractive index layer lies along the radial direction; whereas the negative sign of Δn means that the larger index lies at right angles to the tangential direction. The obtained values for this Δn form follow the negative sign, so the Δn form will, in theory, fall to zero when the refractive index difference between the phases is reduced to zero.

Therefore, to explain different variations in the results, it is essential to take some assumptions into account. Most studies that have involved variations in the physical properties have considered polymers as an anisotropic polycrystalline media, that is, consisting of crystalline regions suspended in a partially oriented amorphous medium.[33] The molecular chains are classified into three structural phases: Δn_c, Δn_a, and Δn_f. These latter classes are insufficient for explaining the results that we obtained. Thus, the use of the suggested subclassification to clarify the

interface distribution of polymer molecular chains was a suitable one and has been widely used to explain isothermal relation results:[15]

1. All thermal structural variations may be considered irreversible at temperatures higher than the glass-transition temperature.
2. The most compact noncrystalline structure is not essentially an orderly structure, and an oriented structure may not be the most compact noncrystalline structure.

When a polymeric fiber was annealed, its structural behavior changed because of the accumulation of several structural processes, which were responses both to annealing temperature and to time[34–37] (shrinkage, crystal decomposition, recrystallization by growth, recrystallization by nucleation, and disorientation).

The results show that changes in ρ occur because of different annealing conditions. Therefore, changes in volume were indicative of the other parameters given in Tables I and II, just as χ_c and ρ were the main parameters in the equations used for evaluation.

The densification process, as a result of annealing, was accompanied by significant changes in the physical and chemical properties. Hence, the overall changes in ρ were important influences on the
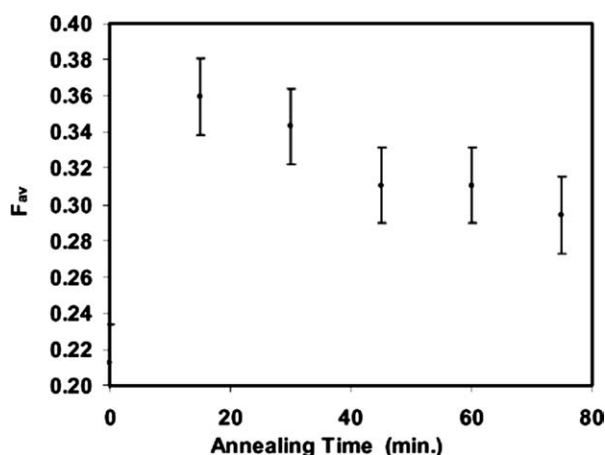

Figure 4 Relationship between F_{av} and the annealing time at a constant annealing temperature for the viscose fibers.
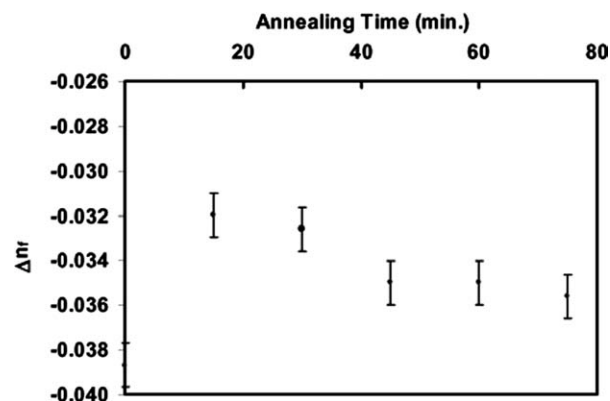

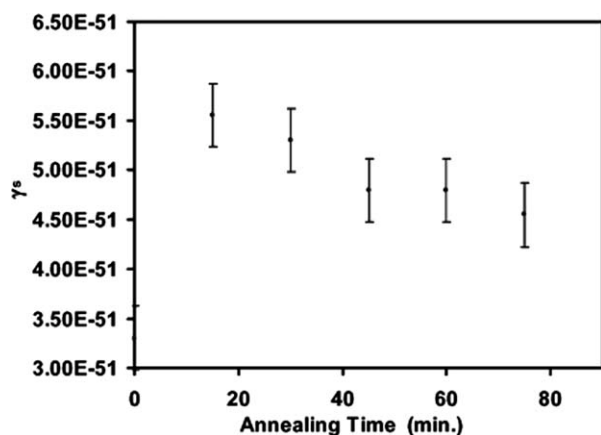**Figure 5** Variation between Δn_f and the annealing time for the viscose fibers.

Figure 6 Change between γ_s and the annealing time for the viscose fibers.

Figure 8 Relation between η_{av} and the annealing time for the viscose fibers.

optical parameters, orientation, χ_c, and so on, as manifested in the results.

The change in fiber ρ was an indication of a change in volume due to the mass redistribution associated with the annealing process. This change in volume affected some other parameters, such as χ, $f(\theta)$, C_s, ε, η, R, and γ_s. These changes may have been the result of an increase in the free volume area spaces, represented in the form of mobile holes jumping around in the structure as a result of thermal treatment. Another means of interpretation would be that the change in the obtained optical parameters may have been the result of the modification of the electrical properties, which arose from the existing space changes and the residual electric field in the polymers after preparation.[38] The change in $\overline{R}$ may have been due to the oxidation factor. In the presence of oxygen, the thermal degradation proceeded by interaction with chemically reactive types of polymers, where, because of thermal annealing in air, surface oxidation could occur. Accordingly, the thermal degradation of textile-
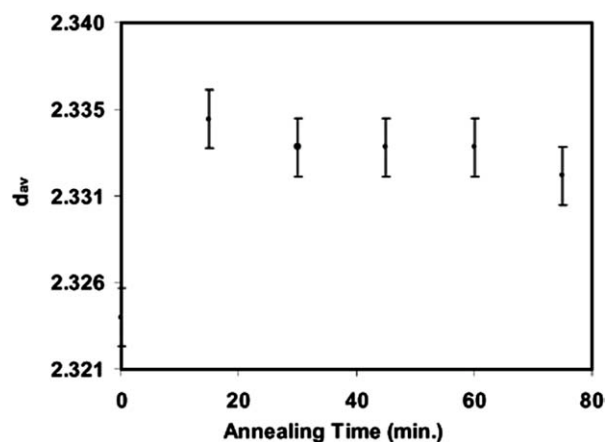
regenerated cellulose was greatly accelerated in the presence of oxygen. This process was coupled with a considerable loss in strength. The oxidation process of cellulose xanthate was also a chain reaction and began at the hydrogen positions to oxidation. The color changes occurring in the presence of air were generally due to oxidation, which started at the surface and gradually penetrated the polymer layers. As the temperature–time intervals of annealing increased progressively, more oxidation occurred.[39]

CONCLUSIONS

It is clear that the two-beam interferometric method is a useful and rapid technique to clarify the optical and ρ parameters of viscose fibers under different thermal conditions. The following conclusions were drawn as a result of the measurements related to the changes in the optical properties, ρ, and χ_c parameters and the thermal effects in the viscose fibers:

1. ρ and χ_c depend greatly on the thermal energy of the intermolecular interactions, which affected the molecular motion in the viscose fibers. Also, these were indicative of the effect of the structural transformation changes on the optothermal parameters of the viscose fibers, as shown in Tables I and II.
2. The value of the calculated Δn_f in Figure 5 increased or decreased for the viscose fibers according to the ratio between the two-phase crystalline and amorphous regions, which depended on the annealing conditions.
3. As the time of annealing increased, there were decreases observed with the optical $[f(\theta)]$'s and γ_s changes, d, η, and $\overline{R}$.
4. It was clear that χ_c depended greatly on the time of annealing because of kinetic changes in

Figure 7 Relation between d_{av} and the annealing time for the viscose fibers.

the chain mobility. These changes threw light on different physical phenomena (swelling, optical, electrical, etc.). The variations in the results due to changes in various parameters could be useful for industrial applications for viscose fibers.

5. The thermal treatment process affected the color of the fibrous materials because of the presence of oxygen, which led to thermooxidative degradation and gave the viscose fibers modified physical properties.

References

1. Heyn, A. N. J. Fiber Microscopy; Interscience: New York, 1954.
2. Fouda, I. M.; Siesa, E. A.; Oraby, A. H. J Appl Polym Sci 1999, 71, 361.
3. Fouda, I. M.; Shabana, H. M. J Appl Polym Sci 2001, 82, 2387.
4. Fouda, I. M.; El-Kodary, A.; El-Sharkawy, F. M. Int J Polym Mater 2007, 56, 965.
5. Fouda, I. M.; Siesa, E. A. J Appl Polym Sci 2007, 106, 1768.
6. Manabe, S.; Iwata, M.; Kamide, K. Polym J 1981, 18, 1.
7. Barakat, N.; Hindelah, A. M. Tex Res J 1964, 34, 357.
8. Barakat, N.; Hindelah, A. M. Tex Res J 1964, 34, 581.
9. Hofmann, D.; Leonhardt, R. P.; Weigel, P. J Appl Polym Sci 1992, 46, 1025.
10. Decandia, F.; Vittoria, .; Petertin, A. J Polym Sci Polym Phy Ed 1985, 23, 1217.
11. Toda, T.; Yoshida, H.; Kunish, K. Fu. Polymer 1997, 38, 5463.
12. Fouda, I. M.; El-Tonsy, M. M. J Mater Sci 1990, 25, 4752.
13. Fouda, I. M.; Shabana, H. M. Polym Polym Compos 2000, 7(7), 51.
14. Zachariodes, A. Z.; Porter, S. The Strength and Stiffness of Polymers; Marcel Dekker: New York, 1983.
15. Fouda, I. M.; El-Tonsy, M. M.; Shaban, A. M. J Mater Sci 1990, 26, 5085.
16. Fouda, I. M.; El-Tonsy, M.; Metawe, F. M.; Hosny, H. M.; Easawi, K. H. J Appl Polym Sci 1997, 66, 695.
17. Fouda, I. M.; El-Tonsy, M. M.; Metawe, F. M.; Hosny, H. M.; Easawi, K. H. Polym Test 1998, 17, 461.
18. Fouda, I. M. Polym Test 2002, 21, 3.
19. Barakat, N.; Hamza, A. A. Interferometry of Fibrous Materials; Hilger: London, 1990.
20. Gedde, U. F. W. Polymer Physics; Chapman & Hall: London, 1997.
21. Hermans, P. H. Contributions to the Physics of Cellulose Fibers; North-Holland: Amsterdam, 1946.
22. Angad Gaur, H.; De Vries, H. J Polym Sci Phys Ed 1975, 13, 835.
23. Murthy, N. S.; Bray, R. G.; Carreale, S. T.; Moore, R. A. F. Polymer 1995, 36, 3863.
24. Happy, F. Applied Fiber Science; Academic: London, 1983.
25. Riande, E.; Guzman, J. J Polym Sci Phys Ed 1984, 22, 917.
26. Wunderlich, B. Macromolecular Physics, Crystal Structure, Morphology, Defects; Academic: London, 1973.
27. Jenkins, A. D. Materials Science Handbook: Polymer Science; North-Holland: Amsterdam, 1972.
28. Hemsley, D. A. Applied Polymer Light Microscopy; Elsevier: London, 1964.
29. De Vries, H. Colloid Polym Sci 1979, 257, 226.
30. Mauersberger, R. H. Mathew's Textile Fibers; Wiley: New York, 1947.
31. Pluta, M. Advanced Light Microscopy; Elsevier: Amsterdam, 1993.
32. Manale, S.; Kamide, R. Text Plach Soc Jpn 1981, 34, 98.
33. Samules, R. J. Structured Polymer Properties; Wiley: New York, 1974.
34. Polukhin, P.; Gorelik, S.; Vortontsov, V. Physical Principal of Plastic Deformation; Mir: Moscow, 1983.
35. Basset, D. C. Principles of Polymer Morphology; Cambridge University Press: Cambridge, England, 1981.
36. Williams, D. J. Polymer Science and Engineering; Prentice-Hall: London, 1971.
37. Fouda, I. M.; Shabana, H. M. Polym Int 1999, 48, 602.
38. Kuleznev, V. N.; Shershnev, V. A. The Chemistry and Physics of Polymers; Mir: Moscow, 1990.
39. Hamza, A. A.; Fouda, I. M.; Kabeel, M. A.; El-Shrif, M.; El-Sharkawy, F. M. Polym Polym Comp 1999, 1, 53.